Symmetry breaking in self-assembled monolayers on solid surfaces. II. Anisotropic substrate elasticity

W. Lu[1] and Z. Suo[2]
[1]*Mechanical Engineering Department, University of Michigan, Ann Arbor, Michigan 48109*
[2]*Mechanical and Aerospace Engineering Department and Princeton Materials Institute, Princeton University, Princeton, New Jersey 08544*
(Received 4 September 2001; published 16 May 2002)

On a solid surface a monolayer mixture may separate into two phases. The phases can self-assemble into a variety of patterns, with the feature size on the scale of 1–100 nm. This paper studies how the elastic anisotropy of the substrate affects the patterns. The substrate is taken to be of cubic crystal symmetry, although the method developed can be readily extended to treat substrates of any other crystalline symmetry. The surface stress differs from one phase to the other, and the difference refines the phases to reduce the elastic energy. The phase boundary energy tends to coarsen the phases. The two competing effects set the phase sizes and the phase patterns. The anisotropy of the substrate elasticity breaks the symmetry of the system. We formulate a phase field model on the basis of this physical picture. The numerical simulation shows that stripes tend to orient along the two compliant directions of the substrate, forming a tweedlike pattern. A square lattice of dots can also be obtained when the anisotropy is weak and the average concentration sufficiently deviates from half filling. We interpret these findings in terms of free energy minimization.

DOI: 10.1103/PhysRevB.65.205418 PACS number(s): 68.43.Hn

I. INTRODUCTION

Experiments have shown for a decade that a monolayer mixture on a solid surface may self-assemble into nanoscale phase patterns. Examples include alternating oxygen and bare copper stripes on the Cu(110) surface,[1] triangular superlattice of S-rich dots in a continuous Ag matrix on the Ru(0001) surface,[2] regular arrays of square islands of N on the Cu(001) surface,[3] and serpentine stripes and triangular lattice of dots of Pb islands on the Cu(111) surface.[4] As discussed in Refs. 5–11, the surface stress varies from one phase to the other. The phases tend to refine to reduce the elastic energy, and coarsen to reduce the phase boundary energy. The two competing effects set the equilibrium phase sizes and the phase patterns.

Unlike the better studied monolayer molecules on an air-liquid interface (i.e., the Langmuir film), the monolayer on a solid surface is usually anisotropic within the plane of the layer. The anisotropy breaks the orientational symmetry, giving rise to diverse phase patterns. At this point, the experimental information available to us on the effects of anisotropy is scanty. This series of papers explore theoretical possibilities within a phase field model that we have developed recently.[7–11]

A monolayer-substrate system can be anisotropic in terms of the surface stress, the elastic constants of the substrate, and the phase boundary energy. In a previous paper,[11] we have investigated the effect of surface stress anisotropy. This paper, the sequel, focuses on the effect of the anisotropy of substrate elasticity. We assume that the substrate is of cubic crystalline symmetry, and the substrate surface coincides with the (001) crystal plane. As will become evident, the method to be developed can be readily extended to treat substrates of any other crystalline symmetry. In this series of papers, we will allow one kind of anisotropy at a time, leaving the interplay among several kinds of anisotropy to future studies. Section II recalls our model for surface patterns. Section III solves the elastic field in the substrate by using the Fourier Transform. Numerical results and discussions are presented in Sec. IV.

II. THE CONTINUOUS PHASE FIELD MODEL

This section outlines the salient features of the model. Refer to our previous papers[7,9] for further details. Consider an epilayer composed of two atomic species A and B on a substrate of atomic species S. A and B can be both different from S, such as the sulfur-silver mixture on the ruthenium substrate.[2] Alternatively, only one atomic species of the epilayer is different from that of the substrate, such as the oxygen atoms on the copper substrate.[1] We model the epilayer as an infinite surface and allow the two species A and B to diffuse within the epilayer. We model the substrate as a semi-infinite elastic body, occupying the half space $x_3<0$ bounded by the x_1-x_2 plane [Fig. 1(a)].

We define the concentration C by the fraction of the atomic sites on the surface occupied by species B. The concentration $C(x_1,x_2,t)$ is a field on the plane (x_1,x_2), evolving with time t as atoms diffuse within the epilayer. Atoms diffuse to reduce the free energy. Within the continuous phase field model, the diffusion equation is

$$\frac{\partial C}{\partial t}=\frac{M}{\Lambda^2}\nabla^2\left(\frac{\partial g}{\partial C}-2h_0\nabla^2 C+\phi\varepsilon_{\alpha\alpha}\right), \tag{1}$$

where M is the mobility of atoms in the epilayer and Λ is the number of atoms per unit area on the surface. The three terms in the bracket in Eq. (1) come from different energetic forces that drive diffusion. The first two terms in Eq. (1), which are analogous to those in Ref. 12, come from the free

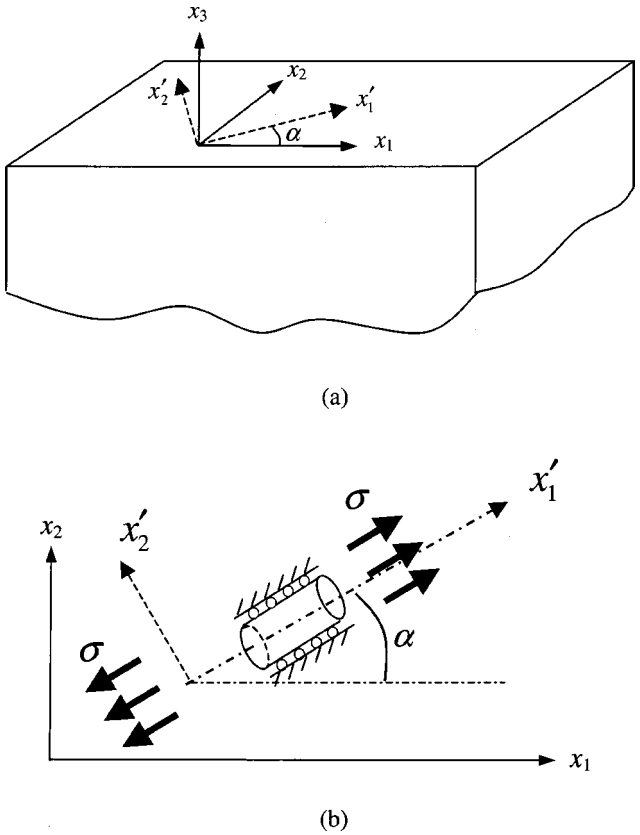

FIG. 1. (a) Illustration of the coordinates. (b) Cut a cylinder along the x_1' direction. The cylinder is constrained so that deformation can only occur along the x_1' direction.

energy of mixing and the phase boundary energy. The third term is due to the concentration-dependent surface stress.

We model the monolayer mixture as a binary regular solution. The free energy of mixing $g(C)$ takes the form

$$g(C)=\Lambda k_B T[C\ln C+(1-C)\ln(1-C)+\Omega C(1-C)], \tag{2}$$

where k_B is Boltzmann's constant and T is the absolute temperature. The dimensionless number Ω measures the enthalpy of mixing in units of the thermal energy $k_B T$. The term $h_0\nabla^2 C$ represents the effect of phase boundary energy, where h_0 is a positive constant.

We assume that the surface stress is a linear function of the concentration, and denote the slope by ϕ. In this paper, the surface stress is taken to be isotropic, so that ϕ is a scalar. $\varepsilon_{\alpha\beta}$ is the elastic strain in the surface. A Greek subscript runs from 1 to 2. A repeated index implies summation. When the concentration field is nonuniform in the epilayer, the surface stress is also nonuniform. The nonuniformity generates a stress field σ_{ij} in the substrate, which is determined by an elasticity boundary value problem. At the surface $x_3=0$, the tractions relate to the concentration as

$$\sigma_{31}=\phi\partial C/\partial x_1,\quad \sigma_{32}=\phi\partial C/\partial x_2,\quad \sigma_{33}=0. \tag{3}$$

The bulk of the substrate is assumed to have cubic crystalline symmetry, with three independent elastic stiffness constants c_{11}, c_{12}, and c_{44}. The surface of the substrate coincides with the (001) crystal plane, and (x_1,x_2,x_3) coincides with the cube edges of the crystal unit cell. The solution of this boundary value problem is given in Sec. III.

When the concentration field is know at a given time, one can compute the driving forces on the right-hand side of Eq. (1) as described above. Equation (1) then updates the concentration for a time step. The procedure is repeated to evolve the concentration field for any finite time. Before describing the numerical method, we first introduce a scheme to normalize the evolution equation. A comparison of the first two terms in the parenthesis in Eq. (1) defines the length

$$b=\left(\frac{h_0}{\Lambda k_B T}\right)^{1/2}. \tag{4}$$

In the Cahn-Hilliard model,[12] this length scales the distance over which the concentration changes from the level of one phase to that of the other, and represents the thickness of the phase boundary.

The other length scale, which reflects the competition between coarsening and refining, is defined by

$$l=\frac{c_{11}h_0}{\phi^2}. \tag{5}$$

This length is obtained by comparing the second and the third terms in the parenthesis in Eq. (1). The feature size of the equilibrium phase pattern is on the order $4\pi l$. The ratio of the two lengths defines a dimensionless parameter $Q=b/l$. This parameter will appear in the normalized equation. The orders of magnitudes of b and l have been estimated in Ref. 9, which broadly agree with the experimental values.

From Eq. (1), disregarding a dimensionless factor, we note that the diffusivity scales as $D\sim Mk_B T/\Lambda$. To resolve events occurring over the length scale of b, the time scale is $\tau=b^2/D$, namely,

$$\tau=\frac{h_0}{M(k_B T)^2}. \tag{6}$$

We solve the evolution equation (1) by the spectral method. This method considerably saves computation time and has been applied to many other problems; see Ref. 13. The elastic field in the half space can be solved analytically by using the Fourier transform. We denote the two-dimensional (2D) Fourier transform of a function $F(x_1,x_2,t)$ by $\hat{F}(k_1,k_2,t)$, where k_1 and k_2 are the coordinates in the reciprocal space. For example, the Fourier transform of the concentration field is

$$\hat{C}(k_1,k_2,t)=\int_{-\infty}^{\infty}\int_{-\infty}^{\infty}C(x_1,x_2,t)e^{-i(k_1x_1+k_2x_2)}dx_1dx_2. \tag{7}$$

Let $k=\sqrt{k_1^2+k_2^2}$, $n_1=k_1/k$, and $n_2=k_2/k$. Normalizing Eq. (1) by the length b and the time τ, and applying the Fourier transform on both sides of the equation, we obtain the evolution equation in the reciprocal space

$$\frac{\partial \hat{C}}{\partial t} = -k^2 \hat{P} - (2k^4 - Qsk^3)\hat{C}. \tag{8}$$

Here $s = -c_{11}\hat{\varepsilon}_{\alpha\alpha}/\phi k\hat{C}$ is a dimensionless function of the elastic constants n_1 and n_2. The expression of s is determined in the next section. $\hat{P}(k_1,k_2,t)$ is the Fourier transform of

$$P(x_1,x_2,t) = \ln\left(\frac{C}{1-C}\right) + \Omega(1-2C). \tag{9}$$

Details about the numerical simulation can be found in Refs. 9, 11, 13.

III. THE ELASTIC FIELD IN A SUBSTRATE WITH CUBIC SYMMETRY

Substrates of cubic crystalline symmetry, such as silicon, silver, gold, and copper, are commonly used in surface studies. It is worthwhile to document the elastic field in such a substrate induced by the nonuniform surface stress. Let u_i be the displacements in the substrate. A Latin subscript runs from 1 to 3. In terms of the displacements, the force balance equation is[14]

$$\begin{aligned}
&c_{11}u_{1,11} + c_{12}(u_{2,21} + u_{3,31}) + c_{44}(u_{1,22} + u_{2,12}) \\
&\quad + c_{44}(u_{1,33} + u_{3,13}) = 0, \\
&c_{44}(u_{1,21} + u_{2,11}) + c_{11}u_{2,22} + c_{12}(u_{1,12} + u_{3,32}) \\
&\quad + c_{44}(u_{2,33} + u_{3,23}) = 0, \\
&c_{44}(u_{1,31} + u_{3,11}) + c_{44}(u_{2,32} + u_{3,22}) + c_{11}u_{3,33} \\
&\quad + c_{12}(u_{1,13} + u_{2,23}) = 0.
\end{aligned} \tag{10}$$

These are three partial differential equations for the displacement field $u_i(x_1,x_2,x_3)$ in the substrate.

Taking the 2D Fourier transform on both sides of Eq. (10), we obtain

$$\begin{aligned}
&R\hat{u}_1'' - (Sk_1^2 + Rk_2^2)\hat{u}_1 - k_1k_2\hat{u}_2 + ik_1\hat{u}_3' = 0, \\
&-k_1k_2\hat{u}_1 + R\hat{u}_2'' - (Sk_2^2 + Rk_1^2)\hat{u}_2 + ik_2\hat{u}_3' = 0, \\
&ik_1\hat{u}_1' + ik_2\hat{u}_2' + S\hat{u}_3'' - R(k_1^2 + k_2^2)\hat{u}_3 = 0,
\end{aligned} \tag{11}$$

where $R = c_{44}/(c_{12} + c_{44})$ and $S = c_{11}/(c_{12} + c_{44})$. The coordinates x_1 and x_2 are transformed to the reciprocal space k_1 and k_2, but x_3 remains untransformed. The prime notation means the differentiation with respect to x_3.

Equation (11) contains a set of linear ordinary differential equations for the functions $u_i(x_3)$. The solution takes the form

$$\hat{\mathbf{u}} = \boldsymbol{\nu} e^{\lambda k x_3}. \tag{12}$$

The constant vector $\boldsymbol{\nu}$ and the constant scalar λ are to be determined. Substituting Eq. (12) into Eq. (11), we obtain

$$\begin{bmatrix} R\lambda^2 - (Sn_1^2 + Rn_2^2) & -n_1n_2 & in_1\lambda \\ -n_1n_2 & R\lambda^2 - (Sn_2^2 + Rn_1^2) & in_2\lambda \\ in_1\lambda & in_2\lambda & S\lambda^2 - R \end{bmatrix} \begin{bmatrix} \nu_1 \\ \nu_2 \\ \nu_3 \end{bmatrix} = \begin{bmatrix} 0 \\ 0 \\ 0 \end{bmatrix}. \tag{13}$$

This is an algebraic eigenvalue problem, λ being the eigenvalue and $\boldsymbol{\nu}$ the eigenvector. To have nontrivial solutions, the determinant of the matrix in Eq. (13) should vanish, leading to

$$\lambda^6 + d_1\lambda^4 + d_2\lambda^2 + d_3 = 0, \tag{14}$$

where

$$\begin{aligned}
d_1 &= -\frac{R^2 + RS + S^2 - 1}{RS}, \\
d_2 &= \frac{R^2 + RS + S^2 - 1}{RS} \\
&\quad + \frac{S^3 - 2RS^2 + (R^2 - 3)S + 2(1+R)}{R^2 S} n_1^2 n_2^2, \\
d_3 &= -\frac{R^2 - 2RS + S^2 - 1}{RS} n_1^2 n_2^2 - 1.
\end{aligned} \tag{15}$$

Equation (14) is a cubic algebraic equation of λ^2, and analytical expressions for the roots can be found in standard mathematical handbooks. The displacements should vanish as $x_3 \to -\infty$. Consequently, we choose the three roots that have positive real part and denote them by λ_1, λ_2, and λ_3. Substituting these eigenvalues back into Eq. (13), we obtain the corresponding three eigenvectors $\boldsymbol{\nu}^{(1)}$, $\boldsymbol{\nu}^{(2)}$, and $\boldsymbol{\nu}^{(3)}$. Each eigenvector is determined up to a scalar. The displacement is a linear combination

$$\hat{\mathbf{u}} = \frac{a_1}{k}\boldsymbol{\nu}^{(1)} e^{\lambda_1 k x_3} + \frac{a_2}{k}\boldsymbol{\nu}^{(2)} e^{\lambda_2 k x_3} + \frac{a_3}{k}\boldsymbol{\nu}^{(3)} e^{\lambda_3 k x_3}, \tag{16}$$

where a_1, a_2, and a_3 are arbitrary constants. The solution (16) satisfies the differential equations in Eq. (11). To determine a_1, a_2, and a_3, we must invoke the boundary conditions.

For the particular problem of this paper, the tractions on the surface $x_3 = 0$ are given by Eq. (3). Taking the 2D Fourier transform, we obtain

$$\hat{\sigma}_{31} = ik_1\phi\hat{C}, \quad \hat{\sigma}_{32} = ik_2\phi\hat{C}, \quad \hat{\sigma}_{33} = 0. \tag{17}$$

To keep the problem general for the time being, let σ_{31}, σ_{32}, and σ_{33} be the arbitrary tractions on the surface. The boundary conditions at $x_3 = 0$ are given by

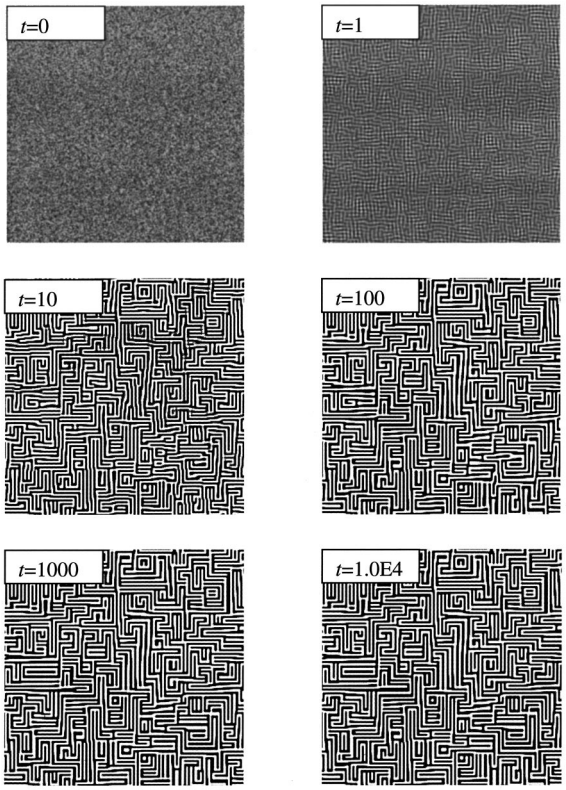

FIG. 2. An evolution sequence on a Cu substrate. The average concentration is 0.5.

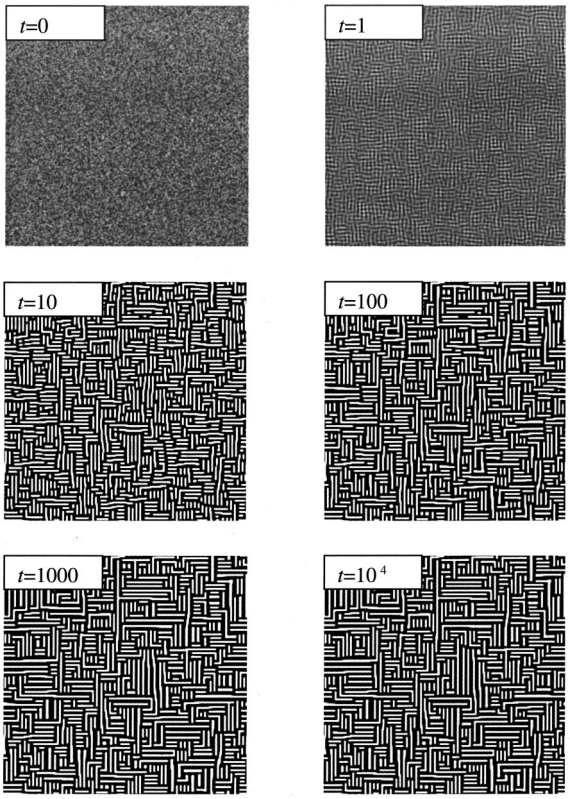

FIG. 3. An evolution sequence on a Cu substrate. The average concentration is 0.4.

$$\sigma_{31}=c_{44}(u_{3,1}+u_{1,3}),$$

$$\sigma_{32}=c_{44}(u_{3,2}+u_{2,3}), \tag{18}$$

$$\sigma_{33}=c_{11}u_{3,3}+c_{12}(u_{1,1}+u_{2,2}).$$

Taking the 2D Fourier transform on the both sides of Eq. (18), we obtain

$$\hat{\sigma}_{31}=c_{44}(ik_1\hat{u}_3+\hat{u}_1'),$$

$$\hat{\sigma}_{32}=c_{44}(ik_2\hat{u}_3+\hat{u}_2'), \tag{19}$$

$$\hat{\sigma}_{33}=c_{11}\hat{u}_3'+c_{12}(ik_1\hat{u}_1+ik_2\hat{u}_2).$$

Substituting Eq. (16) into Eq. (19), we obtain

$$\begin{bmatrix} c_{44}(\lambda_1\nu_1^{(1)}+in_1\nu_3^{(1)}) & c_{44}(\lambda_2\nu_1^{(2)}+in_1\nu_3^{(2)}) & c_{44}(\lambda_3\nu_1^{(3)}+in_1\nu_3^{(3)}) \\ c_{44}(\lambda_1\nu_2^{(1)}+in_2\nu_3^{(1)}) & c_{44}(\lambda_2\nu_2^{(2)}+in_2\nu_3^{(2)}) & c_{44}(\lambda_3\nu_2^{(3)}+in_2\nu_3^{(3)}) \\ c_{12}(in_1\nu_1^{(1)}+in_2\nu_2^{(1)})+c_{11}\lambda_1\nu_3^{(1)} & c_{12}(in_1\nu_1^{(2)}+in_2\nu_2^{(2)})+c_{11}\lambda_2\nu_3^{(2)} & c_{12}(in_1\nu_1^{(3)}+in_2\nu_2^{(3)})+c_{11}\lambda_3\nu_3^{(3)} \end{bmatrix}\begin{bmatrix} a_1 \\ a_2 \\ a_3 \end{bmatrix} = \begin{bmatrix} \hat{\sigma}_{31} \\ \hat{\sigma}_{32} \\ \hat{\sigma}_{33} \end{bmatrix}. \tag{20}$$

Once a_1, a_2, and a_3 are solved from Eq. (20), the displacements are given by Eq. (16). The strain field in the surface $\hat{\varepsilon}_{\alpha\alpha}$ is given by

$$\hat{\varepsilon}_{\alpha\alpha}=ik_\alpha\hat{u}_\alpha. \tag{21}$$

This expression then allows us to calculate s, which in turn enters the evolution equation (8).

As mentioned before, the discrete FFT is used in the numerical simulation. The eigenvalue problem and the value of s at each grid point only need to be computed once, because they only depend on the elastic constants and the position of the grid points in the reciprocal space. Once computed and stored, the values of s at grid points are used in evolving the concentration field at all time. Consequently, the computa-

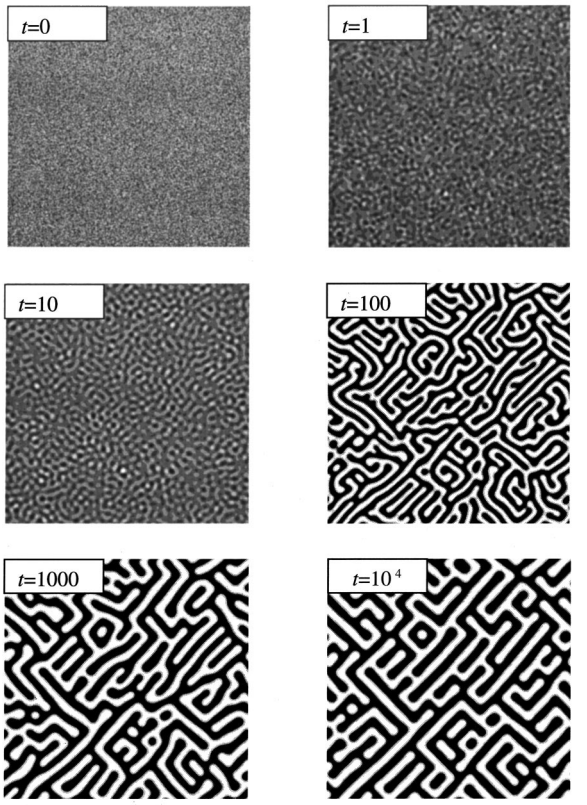

FIG. 4. An evolution sequence on a Mo substrate. The average concentration is 0.5.

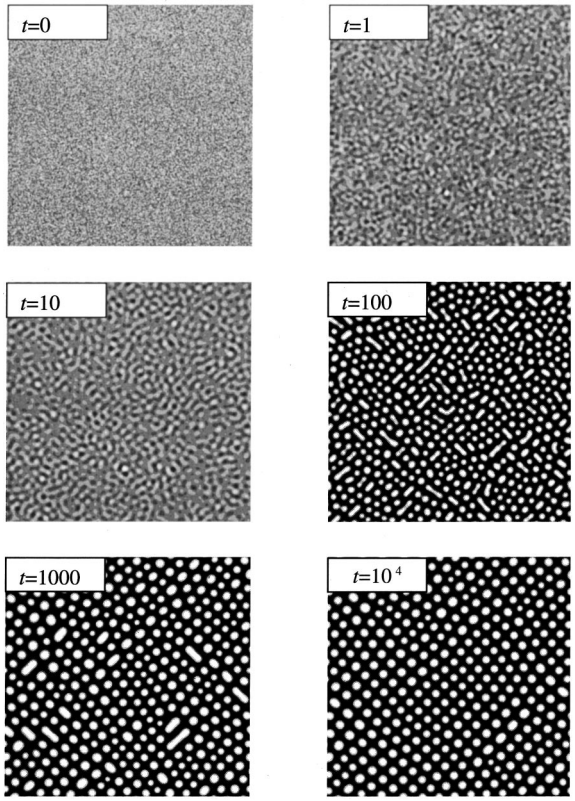

FIG. 5. An evolution sequence on a Mo substrate. The average concentration is 0.4.

tional effort to evolve the concentration field on an anisotropic substrate is nearly the same as that on an isotropic substrate.

IV. NUMERICAL SIMULATIONS AND DISCUSSIONS

In all the simulations reported below, the calculation cell size is $256b \times 256b$, $\Omega = 2.2$, and $Q = 1$. Two crystalline substrates Cu and Mo are used, whose elastic constants are found in standard textbooks. Figure 2 shows a simulated evolution sequence on a Cu(001) surface. The concentration has an average 0.5. The initial concentration fluctuates randomly within 0.001 from the average. It is found that stripes form and line up along the two directions (1,0) and (0,1). The directional preference of the patterns becomes observable at a very early stage, say at $t = 1$. Figure 3 shows another sequence with the average concentration 0.4.

Figure 4 shows an evolution sequence on a Mo substrate. The average concentration is 0.5. The stripes line up along the two directions (1,1) and (−1,1). Figure 5 shows a sequence with average concentration 0.4. In contrast to Cu, a square lattice of dots is obtained for Mo.

The numerical simulations have shown several patterns as above. Consider the stripes at average concentration 0.5. Why do they have different orientations on the substrates of Cu and Mo? How do the orientations relate to the elastic properties of the substrate?

It is well known that the anisotropy of a cubic crystal can be characterized by a single dimensionless parameter

$$\zeta = \frac{c_{12} + 2c_{44}}{c_{11}} - 1. \tag{22}$$

When the crystal is isotropic, $\zeta = 0$. When it is anisotropic, the crystal falls into one of two classes, $\zeta < 0$ or $\zeta > 0$. Note that $\zeta = 0.62$ for Cu, and $\zeta = -0.14$ for Mo. The physical significance of this classification is as follows.

The coordinates (x_1, x_2, x_3) coincide with the three edges of the cubic crystalline cell, as shown in Fig. 1(a). The coordinates (x_1', x_2', x_3') relate to (x_1, x_2, x_3) by a rotation α about the x_3 axis. We cut a cylinder from the substrate along the x_1' direction, as shown in Fig. 1(b). We constrain the cylinder to deform only in the x_1' direction. We denote the stress and strain along this direction by σ and ε, respectively. The stress-strain relation along the x_1' direction is

$$\sigma = c(\alpha)\varepsilon, \tag{23}$$

where

$$\frac{c(\alpha)}{c_{11}} = 1 + \frac{1}{2}\zeta \sin^2 2\alpha. \tag{24}$$

Equation (24) shows that for an anisotropic elastic body, the stiffness measured in a uniaxial strain experiment depends on the orientation.

For the special case of elastic isotropy, $\zeta = 0$, and Eq. (24) gives $c(\alpha) = c_{11}$, independent of the orientation. Figure 6 shows the stiffness versus orientation curve for Cu in the polar coordinate. The distance from a point on the curve to

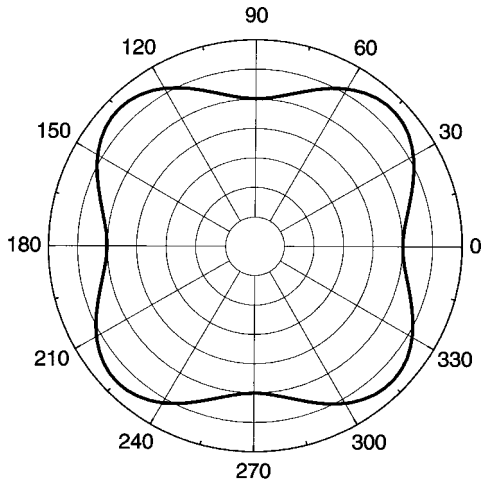

FIG. 6. The stiffness versus orientation curve for Cu in a polar coordinate. $\zeta=0.62$.

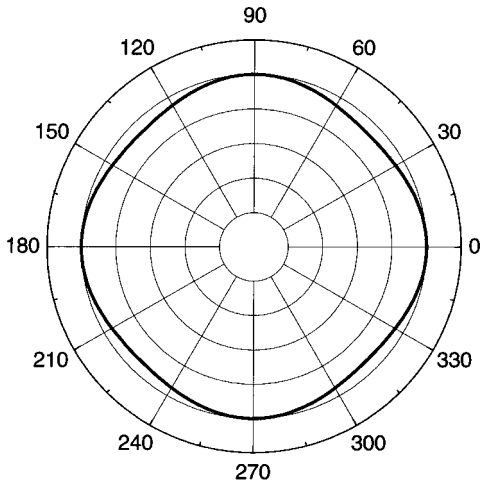

FIG. 7. The stiffness versus orientation curve for Mo in a polar coordinate. $\zeta=-0.14$.

the origin represents the magnitude of stiffness in the direction. A Cu substrate has two compliant directions (1,0) and (0,1) along which the stiffness minimizes. Figure 7 shows the curve for Mo. The two compliant directions are (1,1) and (1,1). It is evident from Eq. (24) that when $\zeta>0$, the compliant directions are (1,0) and (0,1) and when $\zeta<0$, the compliant directions are (1,1) and $(-1,1)$.

Our simulations show that the stripes tend to orient along the compliant directions. This trend can be understood qualitatively. For a fixed stress, the elastic energy density is proportional to the elastic compliance. When the stripes orient along the compliant directions, the system can relax more elastic energy.

Next let us look into the problem in more detail. The question is, assuming that an arbitrary concentration stripe is formed on the substrate, what will the orientation α of the stripe that minimizes the free energy be? The energy per unit area of the system g_{ave} is expressed by[7]

$$g_{\text{ave}}=\frac{1}{A}\int_A\left(g(C)+h_0C_{,\alpha}C_{,\alpha}-\frac{1}{2}\sigma_{3\alpha}u_\alpha\right)dA, \quad (25)$$

where A is the area of the surface and u_α the displacement in the epilayer. In this paper we have assumed that the first two terms in the bracket are isotropic. A calculation shows that for any concentration modulation in the x_1' direction, the free energy takes the form

$$g_{\text{ave}}=g_0+Rg_1, \quad (26)$$

where g_0 and g_1 $(g_1>0)$ are independent of the orientation α, and R depends on α in a special way. Similar to $c(\alpha)$ in Eq. (24), R is an analytical function of ξ, where $\xi=\sin^2 2\alpha$. The preferred orientation is obtained by minimizing g_{ave}, or R. Note that

$$\frac{dR}{d\alpha}=2\frac{dR}{d\xi}\sin 4\alpha. \quad (27)$$

We find R reaches extrema at $\alpha=0$, 45°, 90°, and 135°. Our numerical simulation (including those not reported here) can be distinguished into the following cases.

(i) When $\zeta=0$, the substrate is isotropic. All orientations are energy equivalent, as expected.

(ii) When $\zeta>0$, R minimizes at $\alpha=0$ and $\alpha=90°$. Two energy equivalent variants exist.

(iii) When $\zeta<0$, R minimizes at $\alpha=45°$ and $\alpha=135°$. Two energy equivalent variants exist.

We observe the coexistence of two variants in the numerical simulations shown in Figs. 2 and 4. The two variants form small tweedlike units. The numerical simulation shows that such a configuration is very stable. Although the tweedlike stripes increase the phase boundary energy compared with a set of parallel stripes, it seems that such a configuration reduces more elastic energy. This possibility is being investigated.[15]

At average concentration 0.4, when the substrate is isotropic $(\zeta=0)$, our previous simulation shows that the phases form a lattice of triangular lattice of dots.[9] For Cu $(\zeta=0.62)$, the phases form a tweedlike structure (Fig. 3), probably because the anisotropy is strong. For Mo $(\zeta=-0.14)$, the phases form a square lattice of dots (Fig. 5); the anisotropy apparently is weak enough to allow the dots to form instead of the tweeds, but strong enough to form a square lattice rather than a triangular lattice. Furthermore, on an isotropic substrate, the symmetry makes the triangular lattice in any orientation energy equivalent, leading to a polydomain structure.[9] By contrast, on a cubic substrate, the broken symmetry results in dots in the (1,1) orientation (Fig. 5). However, the cubic crystal only breaks the orientational symmetry, but not the transnational symmetry: dislocations and other imperfections are evident in Fig. 5.

V. CONCLUDING REMARKS

The formation of stable concentration pattern in an epitaxial monolayer requires three ingredients: phase separation, phase coarsening, and phase refining. These ingredients result in a nonlinear diffusion equation, with which we simulated the entire process of pattern evolution. This paper focuses on the effect of substrate elasticity anisotropy on the

pattern formation process. The simulation reveals that the anisotropy of substrate elasticity breaks the symmetry of the system, and tweedlike stripes form along the compliant direction. A square lattice of dots may also be obtained. Crystalline anisotropy only partially breaks the orientational symmetry. Orientational variants (e.g., the tweeds) are still permitted. The square lattice of dots, when formed, are prone to transnational imperfections such as dislocations. To form more ordered structure over a large area, further symmetry breaking operations are necessary, such as using the lithography to define a coarsen patterns on the surface to guide the self-assembly.[10,16] The method developed in this paper can be readily extended to treat substrates with other symmetries, such as the (011) surface of a cubic crystal. For most experimental systems, substrate elasticity, surface stress, and phase boundary can all be anisotropic. One can imagine diverse patterns generated by the interplay of broken symmetries of different kinds. At this point, it begins to be possible to sort out possible patterns within our model. However, the experimental information available to us is so incomplete for any given system that a meaningful comparison with the model is impossible. It is hoped that systematic experiments will soon succeed in bringing out phenomena specific to monolayer mixtures on solid surfaces.

ACKNOWLEDGMENTS

This work was supported by the U.S. Department of Energy through Contract No. DE-FG02-99ER45787.

[1] K. Kern, H. Niebus, A. Schatz, P. Zeppenfeld, J. George, and G. Comsa, Phys. Rev. Lett. **67**, 855 (1991).
[2] K. Pohl, M. C. Bartelt, J. de la Figuera, N. C. Bartelt, J. Hrbek, and R. Q. Hwang, Nature (London) **397**, 238 (1999).
[3] T. M. Parker, L. K. Wilson, and N. G. Condon, Phys. Rev. B **56**, 6458 (1997).
[4] R. Plass, J. A. Last, I.-C. Bartelt, and G. L. Kellogg (unpublished).
[5] O. L. Alerhand, D. Vanderbilt, R. D. Meade, and J. D. Joannopoulos, Phys. Rev. Lett. **61**, 1973 (1988).
[6] K. O. Ng and D. Vanderbilt, Phys. Rev. B **52**, 2177 (1995).
[7] Z. Suo and W. Lu, J. Mech. Phys. Solids **48**, 211 (2000).
[8] W. Lu and Z. Suo, Z. Metallkd. **90**, 956–960 (1999).
[9] W. Lu and Z. Suo, J. Mech. Phys. Solids **49**, 1937 (2001).
[10] Z. Suo and W. Lu, J. Nanopart. Res. **2**, 333 (2000).
[11] W. Lu and Z. Suo, Phys. Rev. B **65**, 085401 (2002).
[12] J. W. Cahn, Acta Metall. **9**, 795 (1961).
[13] L. Q. Chen and Y. Wang, JOM **48**, 13 (1996).
[14] L. D. Landau and E. M. Lifshitz, *Theory of Elasticity* (Butterworth Heimemann, Oxford, 1986).
[15] Y. F. Gao, W. Lu, and Z. Suo (unpublished).
[16] S. Y. Chou and L. Zhuang, J. Vac. Sci. Technol. B **17**, 3197 (1999).